Journal of Glaciology, Vol. 40, No. 134, 1994

Instruments and Methods

Miniature high-power impulse transmitter for radio-echo sounding

B. Barry Narod
Narod Geophysics Ltd, 4413 West 7th Avenue, Vancouver, British Columbia V6R 1X1, Canada

Garry K. C. Clarke
Department of Geophysics and Astronomy, University of British Columbia, Vancouver, British Columbia V6T 1Z4, Canada

ABSTRACT. We have developed a miniature high-power impulse transmitter for radio-echo sounding of glaciers. It features two synchronous second break-down pulse generators operating in a differential configuration. Specifications include bipolar 550 V pulses having rise times less than 2 ns, 512 Hz repetition rate, 180 mA at 10–14 V d.c. operating power, 5 mA standby current and maximum dimension of 12 cm. Because of its small size and low power consumption, the transmitter is suitable for back-portable systems and for towed arrays. The transmitter first saw service in 1990 on Trapridge Glacier, Yukon Territory. Subsequent copies have been used on Agassiz Ice Cap, Northwest Territories, Bering Glacier, Alaska and elsewhere. To date, the maximum ice thickness measured using this transmitter is 825 m, on temperate Bering Glacier.

INTRODUCTION

Impulse radars were introduced to glaciology by Watts and others (1975) and have now become the preferred instrument for ground-based depth sounding of glaciers. The earliest device (Watts and others, 1975; Watts and England, 1976) employed a free-running pulser that used avalanche transistors to provide the signal pulse. This design was proprietory but it seems, in fact, to have been a close relative of a standard circuit published by Andrews (1972). Subsequent improvements to impulse radars have concentrated on increasing the transmitted power, modifying the system for airborne surveys and triggering the transmitter, so that it could be synchronized with a sampler or digitizer. Triggered transmitters have evolved along two lines: those based on avalanche transistors (Watts and Wright, 1981; Wright and others, 1990) and those based on thyristors (Sverrisson and others, 1980; Walford and others, 1986; Jones, 1987; Jones and others, 1989). In this paper, we describe a new transmitter based on avalanche transistors. The transmitter borrows one feature introduced in Jones (1987) and Jones and others (1989): solid-state high-voltage switches are operated in a differential configuration. We believe that this is an important design characteristic, because it appears to promote efficient coupling of the transmitter to its antenna and eliminates the need for a balun. Since 1990, the prototype transmitter has been successfully tested in a wide variety of glaciological settings that range from sub-polar and temperate valley glaciers to a small Arctic ice cap. Our purpose here is to offer the transmitter circuit to others engaged in ice-depth sounding.

TRANSMITTER DESIGN

Figure 1 provides a complete schematic diagram of the pulser. The basic output stage consists of a complementary pair of three-transistor avalanche break-down pulsers (Q1–Q3 and Q4–Q6), more correctly called "current mode second break-down" pulsers (Baker, 1991), that generate symmetric 550 V bipolar steps. The pulsers are triggered simultaneously by current spikes from pulse transformers T1 and T2, which cause one transistor from each string to experience break-down. We constructed a printed circuit board that minimizes path length, inter-trace capacitances and inductances. As a result, the completed transmitter can operate over a wide band of frequencies ranging from 1 to 200 MHz.

Digital logic controls timing. Trigger pulses delivered to the transformers are created either by an on-board crystal oscillator U5, or by light pulses transmitted to an optical receiver U2. Other features include power wake-up circuitry to increase battery life (U4), digital pulse shaping (U4) and voltage regulation (U1 and U3) that allows battery voltages from 10 to 14 V. The high-voltage d.c.–d.c. converter PS1 delivers 1 W at 750 V to the output stage. A system described by Wright and others (1990) has similar attributes. The principal differences in the present design are higher peak RF power (24 kW compared to 10 kW), lower repetition rate (512 Hz compared to 5 kHz) and lower power consumption (2.1 W compared to 22.5 W). Operating battery current is 180 mA and standby current is 5 mA. In 1990, on Trapridge Glacier, one 12 V alkaline lantern battery easily lasted the entire season. For the optical trigger link, we use the Hewlett-Packard plastic fiber "Versatile Link"

https://doi.org/10.3189/S002214300000397X Published online by Cambridge University Press

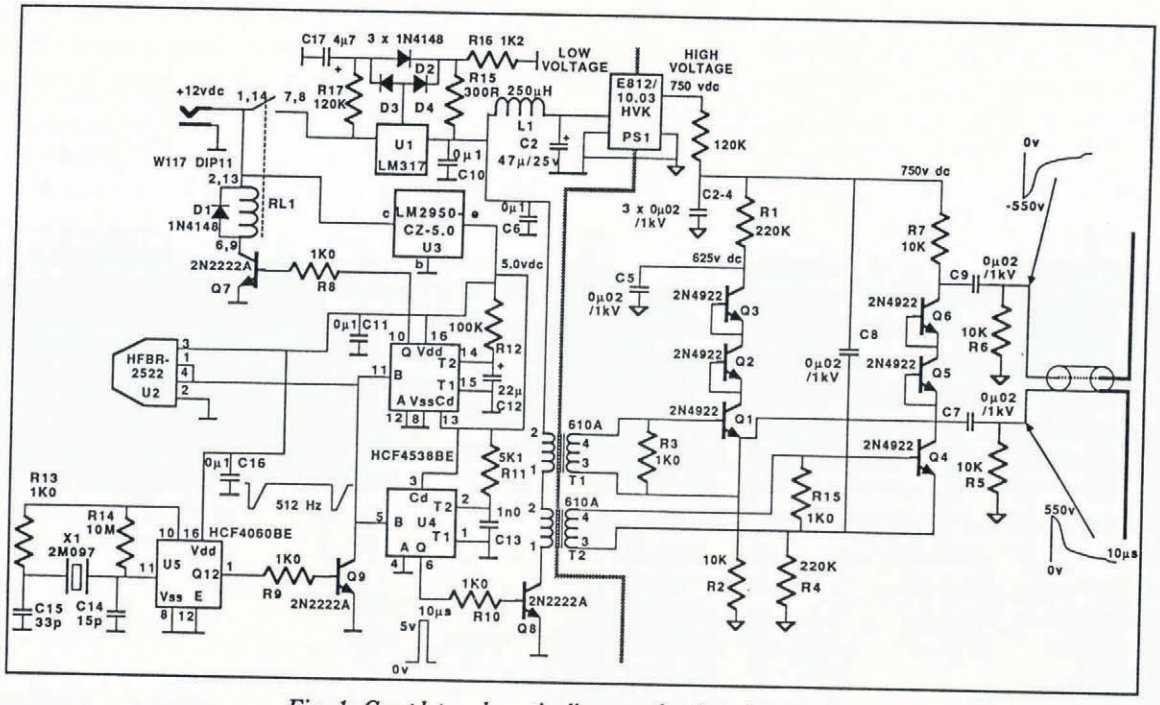

Fig. 1. Complete schematic diagram for the pulse generator.

visible-light system (Hewlett-Packard Company, 1987, p. 8.13–8.36). It has the virtues of being light, compact, inexpensive and mechanically robust.

Table 1. System specification

Pulse characteristics	
Peak power	24 kW, 1.1 kV (± 550 V) into 50 Ω
Rise time	< 2 ns
Repetition rate	512 Hz
Power consumption	
Active	180 mA at 10–14 V d.c.
Standby	5 mA at 10–14 V d.c.
Mechanical	
Dimensions	102 mm × 75 mm × 30mm
Weight	115 g

FIELD TRIALS

Trabant and others (1991) used the new transmitter to obtain spot soundings through as much as 825 m of temperate ice on Bering Glacier, Alaska. Resistively loaded 1 MHz transmitting and receiving antennas were employed and the signal was displayed on an oscilloscope. Unfortunately, the data were not recorded photographically or digitally. Thus, to illustrate capabilities of the new transmitter, we present data from Trapridge Glacier, Yukon Territory, and from Agassiz Ice Cap, Northwest Territories.

Trapridge Glacier, Yukon Territory

Using the new system, we completed an experiment on electromagnetic (EM) wave propagation that relies on the timing stability of our transistor-based pulser and the timing control and EM isolation afforded by the optical link. Theory predicts the existence of interface waves at the ice–air contact. Two of these waves, one propagating at $c_{ICE} \approx 170\,m\,\mu s^{-1}$ and the other at $c_{AIR} = 300\,m\,\mu s^{-1}$, are thought to have $1/r^2$ far-field behaviour (e.g. Annan, 1973; Jezek and others, 1978; Smith, 1984). A third interface wave, propagating at some intermediate

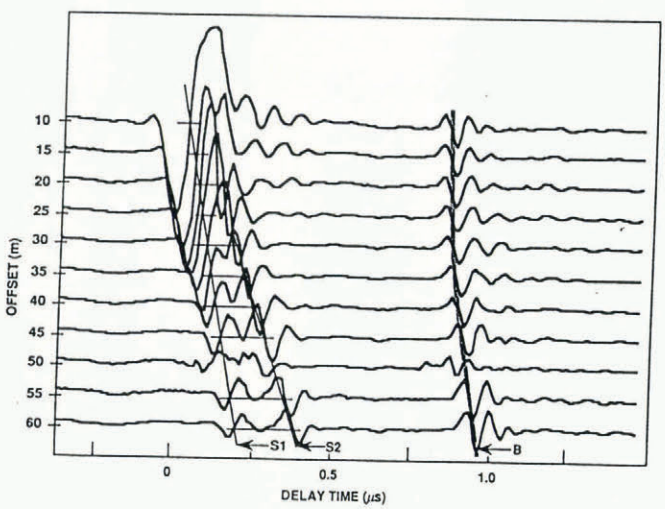

Fig. 2. A common-receiver section taken on Trapridge Glacier using the new pulse generator. Maximum antenna separation was 60 m. The bottom reflection (B) at 70 m has hyperbolic form. The peak amplitude of the reflection is approximately 50 mV into a 50 Ω load. Two direct waves are evident in the section, one travelling through air (S1) at a velocity of 300 m µs^{-1} and one travelling through ice (S2) at 168 m µs^{-1}.

https://doi.org/10.3189/S002214300000397X Published online by Cambridge University Press

velocity, may also exist (personal communication from J. R. Wait) and should have similarities to a Stonely wave (e.g. Ewing and others, 1957, p. 111–12) in acoustics. To our knowledge, this third wave has never been observed in glaciers. Objectives of our field trials on Trapridge Glacier were to seek this wave as well as to study the characteristics of the known ice and air waves.

Figure 2 presents data that were collected on Trapridge Glacier in 1990. This glacier is sub-polar and, in the region studied, the 10 m ice temperature is typically –4°C and the ice thickness is 75 m. The objective was to examine in detail the nature of the EM direct wave which propagates from the transmitter to the receiving antenna and remains near the ice–air interface. For this experiment, the receiver antenna was set at a fixed position, broadside to the transmitter antenna, and the separation distance between antennas was increased in 5 m steps from a minimum separation of 10 m to a maximum of 60 m. We used antennas of 4 m half-length, which gave a centre frequency of 12 MHz. By resistively loading the receiver antenna such that the received signals were halved in amplitude, we determined that the radiation resistance of our antennas was 50 Ω. Our measurements were all made using a 50 Ω receiver antenna load. Data were collected by conditioning the receiver signals using a sampling time base (Jones and others, 1989) and digitizing them to 14 bits using a QSI Corp. C-44 microcontroller. Data were logged on a PC-compatible laptop computer. Use of the optical cable to provide simultaneous triggering of both the receiver and the transmitter ensured accurate relative timing of the recorded wave forms.

In Figure 2, the direct wave, commonly used for receiver triggering, is seen as a complex wavelet in traces of 10 m through 25 m separation. At separations of 30 m or greater, the wavelet can be resolved into two distinguishable wavelets (denoted S1 and S2) travelling at phase velocities of 300 m μs^{-1} and 168 m μs^{-1}, respectively. The former is the expected speed of an electromagnetic wave in air and the latter is the expected speed in ice. The air wave shows a $1/r^2$ attenuation with distance, suggesting that it is losing energy to a head wave in ice as it propagates along the surface. For the air wave, both the propagation velocity and far-field characteristics

Table 2. Transmitter-components list

Identifier	*Part number*	*Part description*
U1	LM317T	Variable-voltage regulator
U2	HFBR-2522	Hewlett-Packard optical receiver (or a 1 kΩ resistor if U2 not installed)
U3	LM2950-CZ-5.0	National semi-conductor 5 V regulator
U4	HCF4538BE	CMOS dual retriggerable one-shot
U5	HCF4060BE	CMOS oscillator/counter
Q1–Q6	2N4922	Motorola NPN transistor
Q7–Q9	PN2222A	NPN transistor
D1–D4	1N4148	Switching diode
R1, R4	220 kΩ	5%, 0.25 W, carbon film
R2, R5–R7	10 kΩ	5%, 0.25 W, carbon film
R3, R8–R10, R13, R15	1.0 kΩ	5%, 0.25 W, carbon film
R11	5.1 kΩ	5%, 0.25 W, carbon film
R12	100 kΩ	5%, 0.25 W, carbon film
R14	10 MΩ	5%, 0.25 W, carbon film
R15	300 Ω	5%, 0.25 W, carbon film
R16	1.2 kΩ	5%, 0.25 W, carbon film
R17	120 kΩ	5%, 0.25 W, carbon film
C1	47 μF/25 V	Aluminium
C2–C5, C7–C9	0.02 μF/1 kV	Ceramic
C6, C10, C11, C16	100 nF	Ceramic
C12	22 μF/25 V	Aluminium
C13	1.0 nF	Ceramic
C14	15 pF	Ceramic
C15	33 pF	Ceramic
C17	4.7 μF	Tantalum
L1	1536X 250 μH	Hammond choke
X1	2.097 MHz	HC-49 crystal
T1, T2	610A or 610AA	Hammond pulse transformer
PS1	E812-10.03 HVK	Endicott Research d.c.–d.c. converter
RL1	W117-DIP11	12 V dual type-C DIP reed delay

https://doi.org/10.3189/S002214300000397X Published online by Cambridge University Press

are consistent with theoretical expectations. Close examination of the ice wave, however, reveals a $1/r$ amplitude attenuation with distance rather than the expected $1/r^2$ dependence. We believe that this observation indicates that present understanding of the EM interface waves is incomplete. The observed $1/r$ dependence is suggestive of radiative propagation in an unbounded medium; evidently, the ice wave resembles a propagating body wave with energy being guided beneath the air–ice surface. Lastly, we find no evidence for the existence of a true surface wave travelling at a velocity intermediate between that of ice and that of air. In a similar experiment, Jezek and others (1978) observed the propagation of an air wave but not that of a direct wave travelling through ice.

Agassiz Ice Cap, Northwest Territories

The low-power consumption, high-peak RF power and compact design make it simple to combine the transmitter with a standard digital oscilloscope and laptop PC to assemble a portable and inexpensive digital radar system. Figure 3 illustrates this capability used for continuous profiling of ice thickness. The data are from a continuous common-offset profile, taken near the summit of Agassiz Ice Cap. In the survey region the 10 m ice temperature is typically –24°C and the ice thickness varies from 150 to 600 m. The data were collected by E. D. Waddington, using a linear transceiver array towed behind a one-person snowmobile. Centre frequency for the antennas was 5 MHz. Data were logged with a Tektronix 222 digital oscilloscope and laptop PC. As in the Trapridge Glacier example, signal quality is high; the transmitter pulse is uncluttered, bottom echoes are sharp and internal layering is clearly revealed without requiring signal enhancement.

CONCLUDING REMARKS

The high performance of the transmitter can, in part, be attributed to careful lay-out of components on the printed circuit board. It is doubtful that a "bread-boarded" rendition would function satisfactorily and careless lay-out of a printed circuit board might also cause problems. Those interested in acquiring copies of our circuit graphics or the board itself are invited to contact us.

Anyone intending to contruct or use the pulse generator described in this paper should be warned that the pulser is capable of causing injury. Even though the mean power consumption is low, the peak power presents a significant RF hazard, capable of causing serious burns. An operating pulser should not be touched on its output terminals and should only be used with an insulated antenna.

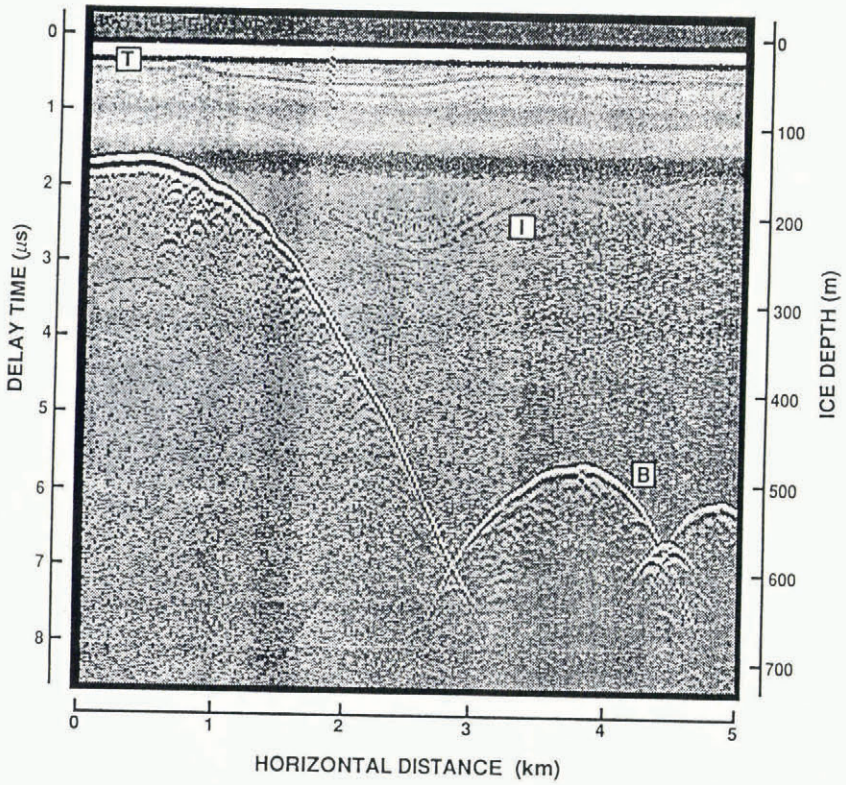

Fig. 3. A common-offset record section taken using the new pulse generator on Agassiz Ice Cap. Centre frequency was 5 MHz. A counter wheel triggered a recording every 22 m of travel, as the antennas and instruments were pulled behind a snowmobile. Total section length is 5.0 km and record duration is 9 μs. An approximate depth scale (right ordinate) is obtained by assuming a constant propagation velocity of 170 m μs^{-1}. The uniform band of energy from 0 to 1.6 μs is the direct wave (T) that propagates from the transmitter antenna to the receiver antenna which were separated by 27 m. Bands of energy (I) offer evidence for internal layering. The bottom reflections (B) ranging from 1.6 to 7.5 μs indicate extreme subglacial topography that produces reflection cusps and diffractions. The near-surface irregularity appearing at 1.8 km is energy scattered from a nearby weather station and its associated cables.

https://doi.org/10.3189/S002214300000397X Published online by Cambridge University Press

ACKNOWLEDGEMENTS

This research was, in part, funded by grants from the Natural Sciences and Engineering Research Council of Canada. We thank Parks Canada and the Yukon Territorial Government for permission to conduct field tests on Trapridge Glacier in Kluane National Park. E. D. Waddington kindly granted permission to use his sounding results from Agassiz Ice Cap.

REFERENCES

Andrews, J. R. 1972. A frequency calibrator for uhf using an avalanche transistor. *QST*, **56**, 16–18.

Annan, A. P. 1973. Radio interferometry depth sounding. Part I—theoretical discussion. *Geophysics*, **38**(3), 557–580.

Baker, R. J. 1991. High voltage pulse generation using current mode second breakdown in a bipolar junction transistor. *Rev. Sci. Instrum.*, **62**(4), 1031–1036.

Ewing, W. M., W. S. Jardetzky and F. Press. 1957. *Elastic waves in layered media*. New York, McGraw-Hill.

Hewlett-Packard Company. 1987. *Optoelectronics designer's catalog 1988–1989*. Palo Alto, CA, Hewlett-Packard Company.

Jezek, K. C., J. W. Clough, C. R. Bentley and S. Shabtaie. 1978. Dielectric permittivity of glacier ice measured *in situ* by radar wide-angle reflection. *J. Glaciol.*, **21**(85), 315–329.

Jones, F. H. M. 1987. Digital impulse radar for glaciology: instrumentation, modelling, and field studies. (M.Sc. thesis, University of British Columbia.)

Jones, F. H. M., B. B. Narod and G. K. C. Clarke. 1989. Design and operation of a portable, digital impulse radar. *J. Glaciol.*, **35**(119), 143–148.

Smith, G. S. 1984. Directive properties of antennas for transmission into a material half-space. *IEEE Trans. Antennas Propag.*, **AP-32**(3), 232–246.

Sverrisson, M., Æ. Jóhannesson and H. Björnsson. 1980. Radio-echo equipment for depth sounding of temperate glaciers. *J. Glaciol.*, **25**(93), 477–486.

Trabant, D. C., B. F. Molnia and A. Post. 1991. Bering Glacier, Alaska—bed configuration and potential for calving retreat. *EOS*, **72**(44), 159.

Walford, M. E. R., M. I. Kennett and P. Holmlund. 1986. Interpretation of radio echoes from Storglaciären, northern Sweden. *J. Glaciol.*, **32**(110), 39–49.

Watts, R. D. and A. W. England. 1976. Radio-echo sounding of temperate glaciers: ice properties and sounder design criteria. *J. Glaciol.*, **17**(75), 39–48.

Watts, R. D. and D. L. Wright. 1981. Systems for measuring thickness of temperate and polar ice from the ground or from the air. *J. Glaciol.*, **27**(97), 459–469.

Watts, R. D., A. W. England, R. S. Vickers and M. F. Meier. 1975. Radio-echo sounding on South Cascade Glacier, Washington, using a long-wavelength, mono-pulse source. *J. Glaciol.*, **15**(73), 459–461.

Wright, D. L., S. M. Hodge, J. A. Bradey, T. P. Grover and R. W. Jacobel. 1990. A digital low-frequency, surface-profiling ice-radar system. *J. Glaciol.*, **36**(122), 112–121.

The accuracy of references in the text and in this list is the responsibility of the authors, to whom queries should be addressed.

MS received 6 May 1992 and in revised form 30 November 1992